Proceedings of the 19th CISM-IFToMM Symposium on Robot Design, Dynamics, and Control, Romansy 2012. pp. 651-656

Modeling Verticality Estimation During Locomotion

Ildar Farkhatdinov [1] Hannah Michalska [2]
Alain Berthoz [3] Vincent Hayward [1]

[1] UPMC Univ Paris 06, UMR 7222,
Institut des Systèmes Intelligents et de Robotique, Paris, France
[2] Department of Electrical and Computer Engineering,
McGill University, Montréal, Qc, Canada
[3] Laboratoire de Physiologie de la Perception et de l'Action,
Collège de France, Paris, France

Abstract Estimation of the gravitational vertical is a fundamental problem faced by locomoting biological systems and robots alike. A robotic model of a vestibular system is suggested with the purpose of explaining an observed phenomenon—head stabilization during locomotion. The mechanical model of the vestibular system comprises a damped inclinometer and an inertial measurement unit which are mounted on an actuated orienting platform (a robotic head). Generic linear control is employed to stabilize the head-platform while the vestibular system exercises an extended Kalman filter algorithm to estimate the gravitational direction in space. It is demonstrated that stabilization of the head-platform is essential in achieving accurate verticality estimation as it attenuates the disturbances generated by locomotion and simplifies state observation in a non-inertial frame, without the need for fixed external beacons.

1 Introduction

Mobile robotic systems including humanoids, mobile robots, or drones typically employ accelerometers and gyrometers packs (known as 'inertial measurement units' or IMU) to obtain information useful for navigation, orientation, balance, attitude control, and other needs, independently from references to external, fixed landmarks [2].

Most humanoids have an IMU attached to their trunk, near the center of mass, to provide balance information [4]. In humans and animals, however, the vestibular system is head-located. This organ is known to serve many functions [1], including gaze stabilization, spatial orientation, and others.

Proceedings of the 19th CISM-IFToMM Symposium on Robot Design, Dynamics, and Control, Romansy 2012. pp. 651-656

It has been proposed by Pozzo and Berthoz [8, 9] that, through head stabilization in orientation, the inertial measurements provided by the vestibular system facilitate the creation of a ground-independent, quasi-inertial, mobile frame from which postural control can be more effectively performed.

With the purpose of clarifying this observation further, a nonlinear mechanical model for gravitational vertical estimation is introduced including an inclinometer combined with an IMU, as proposed in [4]. Here, a more general model of such a robotic vestibular system is presented and the nonlinear gravitational verticality estimation problem is solved using an extended Kalman filter (EKF).

2 Robotic and Human Verticality Estimation

Accelerometers typically report noisy measurements because they pick-up vibrations added to the low frequency components of the signal. Gyroscopic measurements also suffer from bias and are highly sensitive to dynamic errors. To combat these problems, state observers and sensor fusion methods have been proposed [2]. In reference [5], a Kalman filter was used to estimate the vertical direction from tilt measurements in the linearized, planar case. Kalman filters were also applied to attitude estimation of accelerated rigid bodies in three dimensions from fused measurements of gyroscopes and accelerometers [10]. In reference [7], a nonlinear observer for attitude estimation based on gyroscope measurements is described, but only kinematic relationships are considered. A similar problem is solved in [3], where a nonlinear observer combined inertial and visual information is employed. None of these works consider the full system dynamics.

Studies have shown that humans spontaneously stabilize their heads during various locomotion tasks: free walking, walking in place, running in place and hopping [8, 9]. This behavior may reflect the existence of a synergistic interaction between the measurement of rotations by the semi-circular canals and the measurement of translations by the utriculus and sacculus organs. The plane of head stabilization generally is determined by the task and is linked to the gaze direction. At the neural level, it is believed that the estimation of the vertical direction from various sensor inputs is a fundamental brain function and their neural correlates have been studied in humans and animals models [1].

It is an enticing idea to replicate the head stabilization behavior in robots, which is investigated here. Besides suggesting improved robotic design, such replication may provide new insights in the brain functions related to vestibular inputs.

3 Model

Key aspects of the function of the vestibular system can be emulated by a liquid-based inclinometer (Model A900 from Applied Geomechanics). The sensing element is a glass vial partially filled with a conductive liquid, see Figure 1, left panel. When the sensor is level, the four internal electrodes are immersed in the liquid at equal depths; otherwise, the depth of immersion of the electrodes changes, altering the electrical resistance between matched pairs of electrodes. The sensor is mounted on a oriented platform modeled here as a gimble mechanism with two actuators, M1 and M2. A damped pendulum in space with concentrated mass m, viscous damping β and length l, see Fig. 1 right panel, can be used as a mechanical model of the sensor.

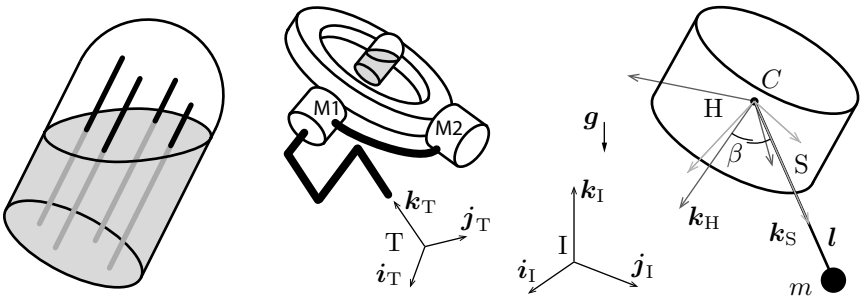

Figure 1. Inclinometer. Left: Liquid partially-filled vial with electrodes. Verticality measurements are affected by fictitious forces when the frame is not Galilean. Middle: actuated gimble mechanism as a model for a head articulated with respect to an arbitrarily moving trunk located by frame T. Frame I is the inertial frame. The platform also supports an IMU (not represented) located near its center. Right: Frame H, in medium gray, is attached to the head and has its origin at C, the center of mass of the platform. Frame S, in light gray, is attached to the pendulum modeled as concentrated mass m located at the end of vector ${}^\mathrm{S}\boldsymbol{l} = [0\ 0\ l]^\top$, aligned with unit vector $\boldsymbol{k}_\mathrm{S}$, having its origin in C, and $\boldsymbol{g}$ is the acceleration of gravity.

In the foregoing, vector and tensor quantities that are sensitive to the frame in which they are expressed receive a left superscript to indicate it. Thus, a rotation transformation written as ${}^\mathrm{B}\mathbf{R}_\mathrm{A}$ is a rotation matrix that transforms, by left multiplication, vectors expressed in frame A into vectors expressed in some frame B. Alternatively, it expresses the orientation of B with respect to A. If B is a frame moving with respect to A and ${}^\mathrm{A}\boldsymbol{q}$ is a position vector expressed in frame A, then $\mathrm{d}^\mathrm{B}\boldsymbol{q}/\mathrm{d}t = \mathrm{d}^\mathrm{A}\boldsymbol{q}/\mathrm{d}t + {}^\mathrm{B}\boldsymbol{\omega}_\mathrm{A} \times {}^\mathrm{A}\boldsymbol{q}$, where

${}^{\mathrm{B}}\boldsymbol{\omega}_{\mathrm{A}}$ is the angular velocity of frame A relatively to B, expressed in frame B. Given a vector $\boldsymbol{q}$, the symbol $[\boldsymbol{q}]_\times$ is used to denote the corresponding skew-symmetric matrix, facilitating differentiation.

The angular momentum of a body, $\boldsymbol{h}$, is the product of a tensor of inertia, $\mathbf{J}$, and an angular velocity, $\boldsymbol{\omega}$, where the angular velocity and the tensor are expressed in the same frame. If the tensor is expressed in a body-fixed frame, the formulae become much simpler since the tensor is constant.

The model requires the definition of four frames: (i) frame I is the inertial frame with unit vectors, $\left\{{}^{\mathrm{I}}\boldsymbol{i}_{\mathrm{I}}, {}^{\mathrm{I}}\boldsymbol{j}_{\mathrm{I}}, {}^{\mathrm{I}}\boldsymbol{k}_{\mathrm{I}}\right\}$; (ii) frame H is the body-fixed head frame with unit vectors, $\left\{{}^{\mathrm{I}}\boldsymbol{i}_{\mathrm{H}}, {}^{\mathrm{I}}\boldsymbol{j}_{\mathrm{H}}, {}^{\mathrm{I}}\boldsymbol{k}_{\mathrm{H}}\right\}$ and with origin at point, C, coinciding with the center of mass of the head; (iii) frame S is the body-fixed pendulum coordinate frame with unit vectors, $\left\{{}^{\mathrm{I}}\boldsymbol{i}_{\mathrm{S}}, {}^{\mathrm{I}}\boldsymbol{j}_{\mathrm{S}}, {}^{\mathrm{I}}\boldsymbol{k}_{\mathrm{S}}\right\}$ such that its $\boldsymbol{k}_{\mathrm{S}}$ axis is aligned with the arm of the pendulum and the pivot coincides with C; (iv) finally, frame T is the frame attached to the trunk of the robot to which the head is attached and that can move in arbitrary ways.

A spherical pendulum is attached to the head which is translated with acceleration ${}^{\mathrm{I}}\boldsymbol{a}$. A torque, ${}^{\mathrm{H}}\boldsymbol{\tau}$, is applied to the head platform by the actuated gimbal. The time derivatives of the angular momenta of the pendulum and of the head are,

$$\dot{\boldsymbol{h}}_{\mathrm{S}} = \frac{\mathrm{d}}{\mathrm{d}t}\left({}^{\mathrm{S}}\mathbf{J}_{\mathrm{S}}\,{}^{\mathrm{I}}\boldsymbol{\omega}_{\mathrm{S}}\right) = {}^{\mathrm{S}}\mathbf{J}_{\mathrm{S}}\,{}^{\mathrm{I}}\dot{\boldsymbol{\omega}}_{\mathrm{S}} + {}^{\mathrm{I}}\boldsymbol{\omega}_{\mathrm{S}} \times {}^{\mathrm{S}}\mathbf{J}_{\mathrm{S}}\,{}^{\mathrm{I}}\boldsymbol{\omega}_{\mathrm{S}},$$

$$\text{and} \qquad \dot{\boldsymbol{h}}_{\mathrm{H}} = \frac{\mathrm{d}}{\mathrm{d}t}\left({}^{\mathrm{H}}\mathbf{J}_{\mathrm{H}}\,{}^{\mathrm{I}}\boldsymbol{\omega}_{\mathrm{H}}\right) = {}^{\mathrm{H}}\mathbf{J}_{\mathrm{H}}\,{}^{\mathrm{I}}\dot{\boldsymbol{\omega}}_{\mathrm{H}} + {}^{\mathrm{I}}\boldsymbol{\omega}_{\mathrm{H}} \times {}^{\mathrm{H}}\mathbf{J}_{\mathrm{H}}\,{}^{\mathrm{I}}\boldsymbol{\omega}_{\mathrm{H}}.$$

The influence of the pendulum on the motion of the head is disregarded, as the mass of the pendulum is considered negligibly small, however, the viscous torque resulting from the difference of the angular velocities of the two bodies must be accounted for. Under these assumptions, the sum of all the moments acting on the pendulum-head system are,

$$\begin{aligned} {}^{\mathrm{S}}\mathbf{J}_{\mathrm{S}}\,{}^{\mathrm{I}}\dot{\boldsymbol{\omega}}_{\mathrm{S}} = &- {}^{\mathrm{I}}\boldsymbol{\omega}_{\mathrm{S}} \times {}^{\mathrm{S}}\mathbf{J}_{\mathrm{S}}\,{}^{\mathrm{I}}\boldsymbol{\omega}_{\mathrm{S}} + mg\,{}^{\mathrm{S}}\boldsymbol{l} \times {}^{\mathrm{S}}\mathbf{R}_{\mathrm{I}}\,\boldsymbol{k}_{\mathrm{I}} \\ &- m\,{}^{\mathrm{S}}\boldsymbol{l} \times {}^{\mathrm{S}}\mathbf{R}_{\mathrm{I}}\,{}^{\mathrm{I}}\boldsymbol{a} - \beta\left({}^{\mathrm{I}}\boldsymbol{\omega}_{\mathrm{S}} - {}^{\mathrm{I}}\boldsymbol{\omega}_{\mathrm{H}}\right), \\ {}^{\mathrm{H}}\mathbf{J}_{\mathrm{H}}\,{}^{\mathrm{I}}\dot{\boldsymbol{\omega}}_{\mathrm{H}} = &- {}^{\mathrm{I}}\boldsymbol{\omega}_{\mathrm{H}} \times {}^{\mathrm{H}}\mathbf{J}_{\mathrm{H}}\,{}^{\mathrm{I}}\boldsymbol{\omega}_{\mathrm{H}} + {}^{\mathrm{H}}\boldsymbol{\tau}. \end{aligned} \tag{1}$$

where ${}^{\mathrm{S}}\mathbf{R}_{\mathrm{I}}\,{}^{\mathrm{I}}\boldsymbol{a}$ is the measurement returned by the IMU's accelerometer. The rates of change of the rotation matrices obey the kinematic relationships,

$$\frac{\mathrm{d}\,{}^{\mathrm{I}}\mathbf{R}_{\mathrm{S}}}{\mathrm{d}t} = \left[{}^{\mathrm{I}}\boldsymbol{\omega}_{\mathrm{S}}\right]_\times {}^{\mathrm{I}}\mathbf{R}_{\mathrm{S}}, \quad \frac{\mathrm{d}\,{}^{\mathrm{I}}\mathbf{R}_{\mathrm{H}}}{\mathrm{d}t} = \left[{}^{\mathrm{I}}\boldsymbol{\omega}_{\mathrm{H}}\right]_\times {}^{\mathrm{I}}\mathbf{R}_{\mathrm{H}}. \tag{2}$$

The inclinometer readings correspond to two angles which describe the orientation of the liquid surface, denoted by a normal vector with respect to

its base. These angles can be expressed through cross products of the corresponding unit vectors of the inclinometer's and head's frame. The outputs of the system comprise the inclinometer readings,

$$\begin{aligned} y_1 &= \arcsin \left\| {}^{\mathrm{I}}\boldsymbol{j}_{\mathrm{H}} \times {}^{\mathrm{I}}\boldsymbol{j}_{\mathrm{S}} \right\| = \arcsin \left\| {}^{\mathrm{I}}\mathbf{R}_{\mathrm{H}}\, {}^{\mathrm{H}}\boldsymbol{j}_{\mathrm{H}} \times {}^{\mathrm{I}}\mathbf{R}_{\mathrm{S}}\, {}^{\mathrm{S}}\boldsymbol{j}_{\mathrm{S}} \right\|, \\ y_2 &= \arcsin \left\| {}^{\mathrm{I}}\boldsymbol{i}_{\mathrm{H}} \times {}^{\mathrm{I}}\boldsymbol{i}_{\mathrm{S}} \right\| = \arcsin \left\| {}^{\mathrm{I}}\mathbf{R}_{\mathrm{H}}\, {}^{\mathrm{H}}\boldsymbol{i}_{\mathrm{H}} \times {}^{\mathrm{I}}\mathbf{R}_{\mathrm{S}}\, {}^{\mathrm{S}}\boldsymbol{i}_{\mathrm{S}} \right\|. \end{aligned} \tag{3}$$

Note that that in steady state inclinometer readings correspond to the head's orientation with respect to the vertical: pitch angle, Θ_x, and roll angle, Θ_y. The IMU's rate gyros measurements are also included in the system's output because they relate directly to the sought unknown states, namely, the head orientation with respect to gravity,

$$\{y_3, y_4, y_5\} = \text{components} \left({}^{\mathrm{H}}\mathbf{R}_{\mathrm{I}}\, {}^{\mathrm{I}}\boldsymbol{\omega}_{\mathrm{H}} \right), \tag{4}$$

which completes the model by collecting (1)–(4). The system states are the elements of the matrices ${}^{\mathrm{I}}\mathbf{R}_{\mathrm{S}}$ and ${}^{\mathrm{I}}\mathbf{R}_{\mathrm{H}}$ and of the vectors ${}^{\mathrm{I}}\boldsymbol{\omega}_{\mathrm{S}}$ and ${}^{\mathrm{I}}\boldsymbol{\omega}_{\mathrm{H}}$.

A crude decentralized 'joint space' control, see [6], is employed to find the motor torques, $\boldsymbol{m} = [m_1, m_2]^{\mathrm{T}}$, that stabilize the head in the horizontal place given an estimate of ${}^{\mathrm{I}}\mathbf{R}_{\mathrm{H}}$. The map, ${}^{\mathrm{T}}\mathbf{R}_{\mathrm{H}} = \Lambda(\theta_1, \theta_2)$, relates the motor shaft angles, $\boldsymbol{\theta} = [\theta_1, \theta_2]^{\mathrm{T}}$, to the orientation of the head with respect to the trunk. The head is horizontal when ${}^{\mathrm{I}}\mathbf{R}_{\mathrm{H}} = {}^{\mathrm{I}}\mathbf{R}(\boldsymbol{k}_{\mathrm{I}})$ where ${}^{\mathrm{I}}\mathbf{R}(\boldsymbol{k})$ represents the rotation about vector $\boldsymbol{k}_{\mathrm{I}}$ that cannot be effected. The orientation ${}^{\mathrm{T}}\mathbf{R}_{\mathrm{H}}$ can be known from the joint angles. If $\theta_1, \theta_2 < \pi/4$, then Λ is invertible and we compute the desired joint angles by solving $\boldsymbol{\theta}_d = \Lambda^{-1}({}^{\mathrm{I}}\mathbf{R}(-\boldsymbol{k}_{\mathrm{I}}){}^{\mathrm{I}}\mathbf{R}_{\mathrm{H}})$. When the servo error is zero, the head orientation, ${}^{\mathrm{I}}\mathbf{R}_{\mathrm{H}} = {}^{\mathrm{I}}\mathbf{R}_{\mathrm{T}}\, {}^{\mathrm{T}}\mathbf{R}_{\mathrm{H}}$, becomes ${}^{\mathrm{I}}\mathbf{R}_{\mathrm{T}}{}^{\mathrm{I}}\mathbf{R}(-\boldsymbol{k}_{\mathrm{I}}){}^{\mathrm{I}}\mathbf{R}_{\mathrm{H}} \Rightarrow {}^{\mathrm{I}}\mathbf{R}_{\mathrm{H}} = {}^{\mathrm{I}}\mathbf{R}(\boldsymbol{k}_{\mathrm{I}})$. The motor torques are obtained from the outputs of proportional-derivative controllers $\boldsymbol{m} = \mathrm{PD}(\boldsymbol{\theta}_d - \boldsymbol{\theta})$ that achieve regulation of $\boldsymbol{\theta}$ to the desired value $\boldsymbol{\theta}_d$. If $\mathbf{M}$ denotes the Jacobian matrix of Λ, ${}^{\mathrm{H}}\boldsymbol{\tau} = \mathbf{M}^{-\mathrm{T}}\boldsymbol{m}$ completes the 'joint space' control action.

4 Extended Kalman Filter

Define a state vector $\boldsymbol{x} = \left({}^{\mathrm{I}}\boldsymbol{\omega}_{\mathrm{S}}\, {}^{\mathrm{I}}\mathbf{R}_{\mathrm{S}}\, {}^{\mathrm{I}}\boldsymbol{\omega}_{\mathrm{H}}\, {}^{\mathrm{I}}\mathbf{R}_{\mathrm{H}} \right)^{\mathrm{T}}$ made of the elements of the vectors where the matrices are arranged in a single vector. The system is then conveniently expressed in the form,

$$\boldsymbol{x}_k = f(\boldsymbol{x}_{k-1}, \boldsymbol{u}_{k-1}, \boldsymbol{w}_{k-1}), \quad \boldsymbol{y}_k = h(\boldsymbol{x}_k, \boldsymbol{\nu}_k),$$

where $\boldsymbol{u} = \left({}^{\mathrm{I}}\boldsymbol{a}\, {}^{\mathrm{H}}\boldsymbol{\tau} \right)^{\mathrm{T}}$ is an input due to the movement of the robot combined with the torque applied to the head. The random variables $\boldsymbol{w}_k$ and $\boldsymbol{\nu}_k$ represent the process and measurement noise. The function f that relates

the state at step $k-1$ to the state at time step k comprises (1) and (2). The output function, h, relates the state $\boldsymbol{x}_k$ to the measurement $\boldsymbol{y}_k$ comprises (3) and (4). Linearizing around an estimate gives,

$$\boldsymbol{x}_k \approx \tilde{\boldsymbol{x}}_k + A(\boldsymbol{x}_{k-1} - \hat{\boldsymbol{x}}_{k-1}) + W\boldsymbol{w}_{k-1}, \boldsymbol{y}_k \approx \tilde{\boldsymbol{y}}_k + H(\boldsymbol{x}_{k-1} - \hat{\boldsymbol{x}}_{k-1}) + V\boldsymbol{\nu}_k.$$

where $\boldsymbol{x}_k$ are the actual state, $\tilde{\boldsymbol{x}}_k$ its estimate, $\boldsymbol{y}_k$ the measurement, $\tilde{\boldsymbol{y}}_k$ its estimate, $\hat{\boldsymbol{x}}_k$ the a posteriori state estimate. The matrices are,

$$A = \frac{\partial f}{\partial \boldsymbol{x}}(\hat{\boldsymbol{x}}_{k-1}, \boldsymbol{u}_{k-1}, \boldsymbol{0}), \qquad W = \frac{\partial f}{\partial \boldsymbol{w}}(\hat{\boldsymbol{x}}_{k-1}, \boldsymbol{u}_{k-1}, \boldsymbol{0}),$$
$$H = \frac{\partial h}{\partial \boldsymbol{x}}(\tilde{\boldsymbol{x}}_k, \boldsymbol{0}), \qquad V = \frac{\partial h}{\partial \nu}(\tilde{\boldsymbol{x}}_k, \boldsymbol{0}).$$

The state update equations are

$$\hat{\boldsymbol{x}}_k^- = f(\hat{\boldsymbol{x}}_{k-1}, \boldsymbol{u}_{k-1}, 0), \qquad P_k^- = A_k P_{k-1} A_k^T + W_k Q_{k-1} W_k^T,$$
$$K_k = P_k^- H_k^T (H_k P_k^- H_k^T + V_k R_k V_k^T)^{-1}, \quad \hat{\boldsymbol{x}}_k = \hat{\boldsymbol{x}}_k^- + K_k(\boldsymbol{y}_k - h(\hat{\boldsymbol{x}}_k^-, 0)),$$
$$P_k = (I - K_k H_k) P_k^-.$$

5 Simulation Results

The parameters were given reasonable values, $m = 50$ g, $l = 0.06$ m, ${}^{\mathrm{S}}\mathbf{J}_{\mathrm{S}} = m\,\mathrm{diag}[l^2, l^2, \frac{1}{20}l^2]$, ${}^{\mathrm{H}}\mathbf{J}_{\mathrm{H}} = \mathrm{diag}[0.125\ 0.125\ 0.125]$ kg·m^2, $\beta = 0.001$ N·ms. The controller was tuned for a critically damped response, with $k_p = 32$ N·m/rad and $K_d = 5$ N·m·s/rad. The sampling period was 1 ms. Estimation was updated every 20 ms. The initial conditions for the EKF differed from that of the system by 0.1 rad. The standard deviation of the process noise, $\boldsymbol{w}_k$, was set to ± 0.001 and that of the measurement noise, $\boldsymbol{v}_k$, to ± 0.02. Moreover, to test robusteness, the model parameters known to the EKF were assumed to differ substancially from the true values, $\tilde{m} = 60$ g, $\tilde{l} = 0.04$ m, ${}^{\mathrm{H}}\tilde{\mathbf{J}}_{\mathrm{H}} = \mathrm{diag}[0.15\ 0.15\ 0.15]$, $\tilde{\beta} = 0.0005$ N·ms.

The tests involved a scenario, `A`, where the head underwent an oscillatory movement which resulted in a three-dimensional trajectory, Fig. 2a. A sudden impact at time 5 s which led to an 30 m/s^2 acceleration spike after which the robot was stopped. In a first condition, the head was rigidly attached to the trunk, that is, ${}^{\mathrm{T}}\mathbf{R}_{\mathrm{H}} = \mathbf{I}$ at all times. In a second the head was stabilized in the horizontal plane using the control outlined earlier. The estimation errors were much smaller when the head was stabilized although the measurement was similarly perturbed.

In another scenario, `B`, the robot jumped in the x-direction as in Fig. 2d. At 'take off' the robot was accelerated in the upward z-direction and at

'landing' the robot experienced an impact from the ground, after which the robot was stopped, Fig. 2d) and (Fig. 2e). The estimation errors were also smaller for the case of horizontally stabilized head. For clarity, the results are presented in Fig. 2 with the noise removed, but noise was present during the simulations.

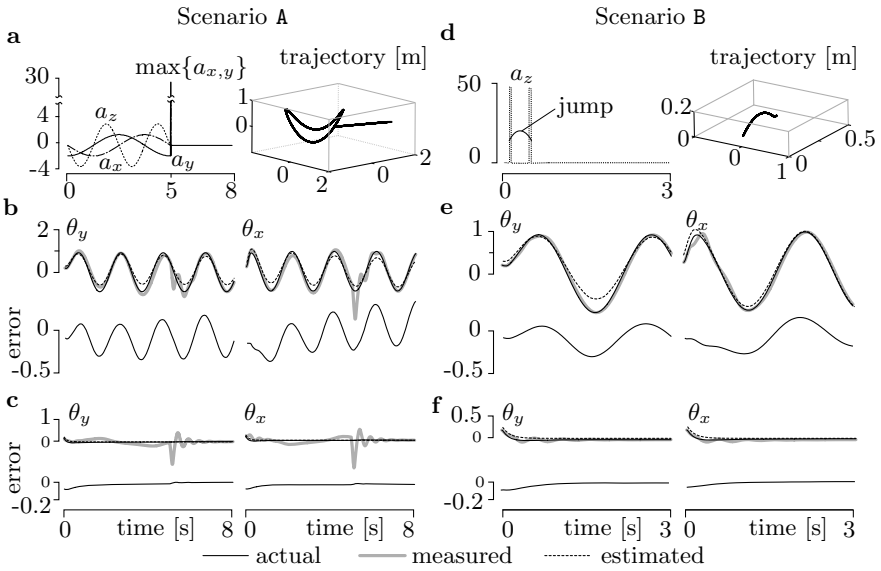

Figure 2. Simulation results. **a**, periodic trajectory and sudden impact at $t = 5\ s$. **b**, non-stabilized head orientation. **c**, stabilized head orientation. **d**, jumping trajectory with two acceleration spikes. **e**, non-stabilized head orientation. **f**, stabilized head orientation. Angles θ_x and θ_y denote the head orientation around $\boldsymbol{k}_\mathrm{I}$ and $\boldsymbol{k}_\mathrm{I}$ respectively.

6 Conclusion and Discussion

Locating the vestibular system in the head has a number of combined advantages, including providing a flexible platform that assists seeking and tracking targets with vision and audition. Here, we developed a dynamic model of what could be called a "robotic vestibular system" comprising a damped inclinometer and an IMU. With this model, we showed that locating the vestibular system in the head enabled inertial stabilization with the consequence of a reduction of the number states to be estimated, while pro-

viding a quasi-inertial reference frame that can facilitate control. We also found that stabilization was especially helpful in the face of uncertainty in the system model. We would like to argue that head stabilization would be of benefit to any robot operating in a non-inertial frame and that such feature should be replicated in their designs.

Bibliography

[1] D.E. Angelaki and K. E. Cullen. Vestibular system: the many facets of a multimodal sense. *Annual Reviews of Neuroscience*, 31:125—150, 2008.

[2] B. Barshan and H. F. Durrant-Whyte. Inertial navigation systems for mobile robots. *IEEE T. on Robotics and Automation*, 11(3):328 –342, 1995.

[3] S. Bras, R. Cunha, J. F. Vasconcelos, C. Silvestre, and P. Oliveira. A nonlinear attitude observer based on active vision and inertial measurements. *IEEE T. on Robotics*, 27(4):664–677, 2011.

[4] I. Farkhatdinov, V. Hayward, and A. Berthoz. On the benefits of head stabilization with a view to control balance and locomotion in humanoids. In *Proc. of the 11th IEEE-RAS Int. Conf. on Humanoid Robots*, pages 147—152, 2011.

[5] J. Leavitt, A. Sideris, and J. E. Bobrow. High bandwidth tilt measurement using low-cost sensors. *IEEE/ASME T. on Mechatronics*, 11(3): 320–327, 2996.

[6] R. P. Paul. *Robot manipulators: mathematics, programming, and control.* MIT Press, 1981.

[7] J. M. Pflimlin, T. Hamel, and P. Souères. Nonlinear attitude and gyroscope's bias estimation for a VTOL UAV. *Int. J. of Systems Science*, 38(3):197–210, 2007.

[8] T. Pozzo, A. Berthoz, and L. Lefort. Head stabilisation during various locomotor tasks in humans. *Experimental Brain Research*, 82(1):97–106, 1990.

[9] T. Pozzo, Y. Levik, and A. Berthoz. Head and trunk movements in the frontal plane during complex dynamic equilibrium tasks in humans. *Experimental Brain Research*, 106(2):327–338, 1995.

[10] H. Rehbinder and X. Hu. Drift-free attitude estimation for accelerated rigid bodies. *Automatica*, 40(4):653—659, 2004.